Biochimica et Biophysica Acta 1808 (2011) 761–773

Contents lists available at ScienceDirect

Biochimica et Biophysica Acta

journal homepage: www.elsevier.com/locate/bbamem

Myelin basic protein binds microtubules to a membrane surface and to actin filaments in vitro: Effect of phosphorylation and deimination

Joan M. Boggs [a,c,*], Godha Rangaraj [a], Yew-Meng Heng [b], Yuanfang Liu [a], George Harauz [d]

[a] Molecular Structure and Function Program, Research Institute, the Hospital for Sick Children, Toronto, ON, Canada M5G 1X8
[b] Department of Paediatric Laboratory Medicine, the Hospital for Sick Children, Toronto, ON, Canada M5G 1X8
[c] Department of Laboratory Medicine and Pathobiology, University of Toronto, Toronto, ON, Canada M5G 1L5
[d] Department of Molecular and Cellular Biology, and Biophysics Interdepartmental Group, University of Guelph, Guelph, ON, Canada N1G 2W1

ARTICLE INFO

Article history:
Received 9 November 2010
Received in revised form 15 December 2010
Accepted 16 December 2010
Available online 23 December 2010

Keywords:
Intrinsically disordered protein
Polyanion
Cytoskeleton
Liposome
Oligodendrocyte
Citrulline

ABSTRACT

Myelin basic protein (MBP) is a multifunctional protein involved in maintaining the stability and integrity of the myelin sheath by a variety of interactions with membranes and other proteins. It assembles actin filaments and microtubules, can bind actin filaments and SH3-domains to a membrane surface, and may be able to tether them to the oligodendrocyte membrane and participate in signal transduction in oligodendrocytes/myelin. In the present study, we have shown that the 18.5 kDa MBP isoform can also bind microtubules to lipid vesicles in vitro. Phosphorylation of MBP at Thr94 and Thr97 (bovine sequence) by MAPK, and deimination of MBP (using a pseudo-deiminated recombinant form), had little detectable effect on its ability to polymerize and bundle microtubules, in contrast to the effect of these modifications on MBP-mediated assembly of actin. However, these modifications dramatically decreased the ability of MBP to tether microtubules to lipid vesicles. MBP and its phosphorylated and pseudo-deiminated variants were also able to bind microtubules to actin filaments. These results suggest that MBP may be able to tether microtubules to the cytoplasmic surface of the oligodendrocyte membrane, and that this binding can be regulated by post-translational modifications to MBP. We further show that MBP appears to be co-localized with actin filaments and microtubules in cultured oligodendrocytes, and also at the interface between actin filaments at the leading edge of membrane processes and microtubules behind them. Thus, MBP may also cross-link microtubules to actin filaments in vivo.

1. Introduction

Myelin basic protein is an intrinsically disordered, or conformationally adaptable, protein that acquires structure on binding to different ligands [1,2]. Like other intrinsically disordered proteins such as synuclein, MARCKS (myristoylated alanine-rich C kinase substrate), histones, and a variety of microtubule associated proteins (MAPs) [3], it may have a number of functions [2,4]. Its primary role is to bind to negatively-charged lipids at the cytoplasmic surfaces of myelin and cause adhesion of these surfaces. However, it also binds to a number of other proteins such as Ca^{2+}-calmodulin [5–7], actin [6–8], tubulin [9,10], and SH3-domain proteins [11]. It causes actin polymerization and bundling [6–8], and it binds actin filaments and the SH3-domain of Fyn tyrosine kinase to lipid bilayers [6,11–14]. Thus, MBP may serve as a scaffolding protein that binds other proteins to the cytoskeleton and to the cytoplasmic surface of the plasma membrane.

There is abundant evidence from a number of groups that MBP also interacts with microtubules both in vitro and in vivo. Similar to its effects on actin, it causes tubulin polymerization and bundles microtubules [9,10]. It stabilizes microtubules from depolymerizing in the cold in vitro, and in cultured oligodendrocytes (OLs) [15,16]. These activities are inhibited by Ca^{2+}-calmodulin (CaM). MBP co-localizes with microtubules in OLs [17–19], and co-immunoprecipitates with tubulin from brain tissue [20]. A recent proteome analysis of microtubule-associated proteins from mammalian brain identified MBP as one of them [21]. It is recovered, together with tubulin, in

Abbreviations: bC1, C1 isolated from bovine brain; bC1-P, bC1 phosphorylated *in vitro* by MAPK; C1, naturally occurring, least modified, most positively-charged component of 18.5 kDa MBP; C2, C3, C4, C5, C6, other naturally occurring charge components of MBP successively differing in charge by −1 due to various post-translational modifications; C8, least positively-charged component of MBP with 6 Arg replaced by citrulline; CaM, calmodulin; F-tubulin, fluorescein-labeled tubulin; GFP, green fluorescent protein; LUVs, large unilamellar vesicles; MAP, microtubule-associated protein; MAPK, mitogen-activated protein kinase; MARCKS, myristoylated alanine-rich C kinase substrate; MBP, myelin basic protein; OLs, oligodendrocytes; rmC8, His-tagged recombinant analogue of murine C8 with 6 Arg/Lys replaced by glutamine; PC, phosphatidylcholine; PG, phosphatidylglycerol; R-actin, rhodamine-labeled actin; RFP, red fluorescent protein; TEM, transmission electron microscopy

* Corresponding author. Molecular Structure and Function Program, Research Inst., the Hospital for Sick Children, 555 University Ave., Toronto, ON, Canada M5G 1X8. Tel.: +1 416 813 5919; fax: +1 416 813 5022.
E-mail address: jmboggs@sickkids.ca (J.M. Boggs).

0005-2736/$ – see front matter © 2010 Elsevier B.V. All rights reserved.
doi:10.1016/j.bbamem.2010.12.016

detergent-insoluble extracts from myelin [22–25]. Studies of cultured OLs isolated from the *shiverer* mutant mouse, in which MBP is lacking, support an important role for interaction of MBP with microtubules and/or actin filaments in myelination [26]. In cultured OLs from this mutant mouse, the microtubules and actin filaments were abnormal in size and distribution, and production of processes and membrane sheets was abnormal. The inability of this mutant to form central nervous system myelin demonstrates the importance of MBP to myelin production, and interactions with the cytoskeleton may play a role.

In the present study, we investigate the ability of MBP to tether microtubules to lipid bilayers and to actin filaments in vitro, and the effects of post-translational modifications to MBP on these interactions. Phosphorylation of MBP in OLs and in myelin occurs at a number of Ser/Thr sites during signaling events and during nerve action potentials [27–31]. Deimination of Arg to citrulline occurs most frequently at 6 sites [32], with the deiminated form being highest in children, indicating a physiological role in myelination. However, deimination of MBP increases in adult MS patients, suggesting that it may also have a pathological role [33,34]. Peptidyl-bound citrulline is uncharged; thus, both of these modifications decrease the net positive charge of MBP, and affect its interactions with many negatively-charged ligands. We show here that MBP can tether microtubules to a lipid bilayer and to actin filaments. Using MBP phosphorylated in vitro at Thr94 and Thr97 (bovine sequence) by MAPK (mitogen-activated protein kinase), and recombinant murine pseudo-deiminated MBP in which the six deiminated Arg are replaced by glutamine, we show that these modifications greatly reduce the ability of MBP to tether microtubules to the negatively-charged lipid bilayer.

2. Materials and methods

2.1. Materials

Naturally occurring MBP migrates as several bands on alkaline gels due to charge components termed C1, C2, C3, C4, and C5. They can be fractionated by carboxymethyl cellulose chromatography at alkaline pH. Components C3 and C5 differ from C1 by an increase in negative charge of −2 and −4, respectively, due to various post-translational modifications, including phosphorylation. Here, the least modified, most highly positively-charged 18.5 kDa component, bC1, was purified from bovine brain MBP as described [35]. It was phosphorylated with recombinant p42 MAPK (New England Biolabs) as described previously [12]. This procedure results in phosphorylation of MBP at both Thr94 and Thr97 to varying degrees of completion. The preparations were run on alkaline-urea tube gels resulting in varying proportions of two bands that migrated similarly to the natural purified MBP charge components, C3 and C5 [12]. Mass spectrometry showed that preparations migrating like C5 had 2 mol of phosphate per mol of MBP. All of the studies reported in this paper were carried out with a preparation containing both mono- and di-phosphorylated bC1, but the latter was the predominant species.

A naturally occurring charge component C8, in which six or more Arg are deiminated to Cit, does not enter the alkaline gel and elutes from the carboxymethyl cellulose column in the void volume. Since the naturally occurring C8 component is not abundant in bovine brain, the pseudo-deiminated recombinant murine form, in which the six deiminated Arg found in the naturally occurring charge component C8 are replaced by Gln, giving rmC8, was prepared as described [36]. It contains an LEH_6 tag, but the His should not be protonated at the pH of the buffers used in this study. The recombinant form, rmC8 has been shown by experimental and modelling studies to be an excellent analogue of natural C8 in most respects [5,36,37].

Egg L-α-phosphatidylcholine (PC) was purchased from Sigma (St. Louis, MO). L-α-phosphatidylglycerol (PG; prepared from egg PC) was obtained from Avanti Polar Lipids, Inc. (Alabaster, AL). [^{3}H]-cholesterol was from GE Health Care (Baie d'Urfe, QC, Canada). Phospholipid concentrations of stock solutions in solvent were determined by phosphorous analysis.

Monomeric tubulin, paclitaxel-stabilized microtubules, fluorescein-labeled tubulin (F-tubulin), G-actin, rhodamine-labeled actin (R-actin), and paclitaxel were purchased from Cytoskeleton (Denver, CO), and stored lyophilized at −80 °C. The Na_2ATP (grade 1) was purchased from Sigma (St. Louis, MO). The GTP was from Roche Applied Science (Laval, QC, Canada). Rabbit anti-actin antibody was purchased from Sigma (St. Louis, MO), rabbit polyclonal anti-MBP antibody (E5), IgG fraction, was a gift from Dr. E. Day [38], and goat anti-rabbit IgG conjugated to HRP (horseradish peroxidase) was purchased from Jackson ImmunoResearch Labs (West Grove, PA). The enhanced chemiluminescence ECL™ Western Blotting reagents were from GE Health Care. Rabbit anti-α/β-tubulin antibody was from Cell Signaling Technology (Beverly, MA).

2.2. Tubulin polymerization

Tubulin polymerization was measured by light scattering using a fluorimeter with excitation and emission wavelengths set at 340 nm, a slit width of 1 mm, and cuvette holder maintained at 37 °C. The GPEM buffer (80 mM PIPES-KOH, 2 mM $MgCl_2$, 0.5 mM EGTA, 1 mM GTP, pH 6.9) was added to each vial of tubulin (with no additives) to give a concentration of 1 mg tubulin/150 μL, and left on ice for 5 min. It was mixed with a pipette and the contents of several vials were pooled, as required for the experiment, and kept on ice until use. The MBP variants were dissolved in GPEM at a concentration of 18.5 μg/160 μL. Polymerization was induced by the addition of 440 μg tubulin in 66 μL to 334 μL of MBP samples (diluted with additional GPEM in a cuvette). The final concentration of tubulin was 20 μM, and the mole ratio of MBP to tubulin was varied from 1:4 to 1:16. Other buffers tried were GPEM without $MgCl_2$ and EGTA, and 20 mM sodium phosphate at pH 6.9 containing 1 mM GTP, with and without 2 mM $MgCl_2$ and 0.5 mM EGTA [39]. All additives and buffers were pre-warmed to 37 °C, and the MBP and additional GPEM were combined first before addition of the cold tubulin solution. The sample was mixed gently by inversion, and immediately placed in the spectrometer for measurement of emission over time, at 37 °C.

2.3. Determination of interaction of tubulin and MBP variants with large unilamellar vesicles (LUVs)

Extruded LUVs containing PC/PG 8.5/1.5 or 9/1 (mol/mol) and trace amounts of [^{3}H]-cholesterol as a marker (final specific activity of 200,000 dpm/10 μmol of phospholipid) were prepared in modified GPEM buffer with the $MgCl_2$ and GTP omitted, at a final concentration of 6 mg lipid or 7.8 μmol/350 μL as described previously [6,13]. Paclitaxel-stabilized microtubules, as supplied by the manufacturer, were used; 150 μL GPEM was added to each vial containing 500 μg tubulin, and the pellet was left on ice 3 min to soften and then mixed with a pipette to dissolve. An additional 100 μL GPEM was added to each vial and the contents of several vials were pooled, as required for the experiment, and kept on ice until use. The paclitaxel-stabilized microtubules were added to MBP variants with or without LUVS in GPEM, usually with no additional paclitaxel. However, in some cases the GPEM added to the vial contained 20 μM paclitaxel, final samples with LUVs and MBP contained 2 μM paclitaxel, and the 40% sucrose layer contained 2 μM paclitaxel. Preliminary experiments showed that use of paclitaxel-stabilized microtubules decreased the amount of tubulin found in the buffer layer after centrifugation (not shown). However, 2 μM paclitaxel was usually not included in either the buffer or the sucrose layer since it seemed to interfere with the protein assay. Moreover, paclitaxel was not necessary to maintain polymerization of most of the tubulin if MBP was present. An amount of 40.3 μg (2.2 nmol) MBP component in 160 μL GPEM was added to 120 μL

GPEM solution containing 240 μg tubulin (4.4 nmol), and incubated for 15 min at 37 °C. The LUVs (600 μg) plus 117 μL GPEM were then added to a final volume of 437 μL, and incubated for a further 5 min at 37 °C. An aliquot was removed for analysis of the initial mixture; the remainder was placed on 500 μL of 40% sucrose made in GPEM in an Eppendorf tube, and centrifuged in a bench-top centrifuge at 14,000 *g* for 60 min, at room temperature.

Preliminary experiments showed that the LUVs with only MBP added formed a band within the buffer layer, whereas LUVs that bound both MBP and tubulin formed an opaque white band on top of the 40% sucrose layer (Fig. 1). The MBP/tubulin complex, without lipid sedimented to the bottom of the tube. However, microtubules by themselves did not, even in the presence of 2 μM paclitaxel. The LUVs alone, and MBP alone, also do not sediment under these conditions [13]. The position and appearance of the bands were noted. Any visible opaque bands were collected separately, and buffer and sucrose layers above and below the bands were also collected separately. After removal of most of the 40% sucrose layer, the bottom of the tube was washed out with buffer to collect any pellet at the bottom. Aliquots of each fraction were taken for [^{3}H]-cholesterol counting, protein assay, running on gels, and analysis of MBP by slot blots.

2.4. Protein analysis

Total protein was assayed by the BioRad assay (BioRad, Hercules, CA). Aliquots for gels were lyophilized and taken up in 2% SDS (sodium dodecyl sulfate). Samples were run on NuPage Bis–Tris 10% polyacrylamide gels (Invitrogen, Carlsbad, CA) with known amounts of MBP and tubulin standards. Coomassie blue-stained gels were analyzed with a UVP image analyzer (UVP, Upland, CA), and band areas were related to those of the standards in order to quantify the amount of each protein in the sample as described [6]. The amount of MBP in the samples was confirmed by slot blots as described [12].

2.5. MBP-mediated interaction of fluorescent actin filaments and microtubules

The ability of MBP variants to bind fluorescently-labeled actin filaments and microtubules to each other was determined by confocal microscopy, as described by Tsukada et al. [40] with some modifications. The R-actin (20 μg) was reconstituted in 40 μL G-actin buffer containing 5 mM Tris, 0.2 mM $CaCl_2$, at pH 8 by incubation for 30 min on ice. Then 4 μL of 10× actin polymerization buffer (5 mM Tris, 500 mM KCl, 20 mM $MgCl_2$, and 10 mM ATP, pH 8) was added and the sample was incubated for 1 h at room temperature. The F-tubulin (20 μg) was reconstituted by addition of 12 μL of GPEM containing 5% glycerol, and incubated for 3 min at 37 °C. Polymerization was induced by addition of 1 μL DMSO (dimethyl sulfoxide) and incubation proceeded at 37 °C for 30 min. Then 2.3 μL of 200 μM paclitaxel was added to stabilize the microtubules. The R-actin filaments were diluted 1/10 in F-buffer containing 5 mM Tris–HCl, 0.2 mM $MgCl_2$, 50 mM KCl, 0.2 mM $CaCl_2$, 1 mM Na_2ATP at pH 8, with or without the addition of MBP variant. The F-microtubules were diluted 1/10 in GPEM buffer containing 20 μM paclitaxel, with or without the addition of MBP component. For mixtures of R-actin filaments and F-microtubules, 1/5 diluted samples of each were combined with or without the addition of MBP component at mole ratios of actin:tubulin:MBP of 1:2:1, 1:2:2, 1:2:5, and 1:4:2. The samples were loaded on a slide, covered with a cover-slip, sealed around the edges with clear nail polish, and examined with a Zeiss confocal laser-scanning microscope with LSM510 software.

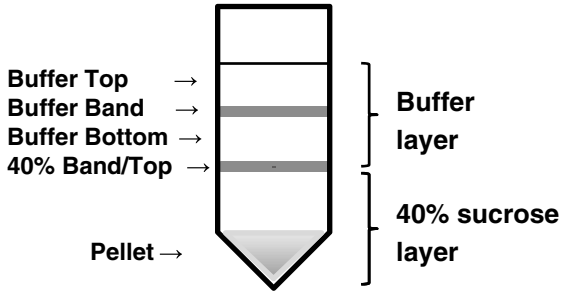

Fig. 1. Large unilamellar vesicles (LUVs) with MBP and/or microtubules were centrifuged in an Eppendorf tube on a 40% sucrose cushion in order to separate any tubulin–MBP complex not bound to lipid from a lipid-bound MBP–tubulin complex, and from MBP–lipid or protein-free lipid vesicles. The position and appearance of any visible opaque bands were noted and they were collected separately (buffer band, 40% band). The buffer and sucrose layers above and below the bands (buffer top, buffer bottom, 40% top [collected separately even if no band was seen], and 40% layer) were also collected separately. The LUVs plus MBP were found as a diffuse band in the buffer layer (buffer band and buffer bottom). In the presence of paclitaxel-stabilized microtubules, most of the bC1 and tubulin were found bound to LUVs in an opaque band on top of the 40% sucrose layer (40% band). The MBP/tubulin complex without lipid sedimented as a visible pellet through the 40% sucrose to the bottom of the tube (pellet).

2.6. Transmission electron microscopy (TEM)

Paclitaxel-stabilized microtubules in the presence or absence of MBP variants and LUVs prepared as described above, with or without additional paclitaxel, were used for transmission electron microscopy (TEM) either before or after centrifugation on 40% sucrose. A 5 μL droplet of each sample was pipetted onto a Formvar-coated grid and negatively-stained with 2% uranyl acetate. In addition, samples for TEM were prepared by addition of LUVs to MBP-bound microtubules already adsorbed to the grid [41]. Paclitaxel-stabilized microtubules were prepared as described above and combined with MBP variant at a 2:1 mole ratio of tubulin:MBP and a final concentration of 30 μg tubulin/55 μL, and incubated at 37 °C for 30 min. A 5 μL aliquot was applied to the grid, allowed to adsorb for 3 min, and then 5 μL LUVs (containing 8.9 μmol lipid) was added to the grid and allowed to adsorb for 3 min. The grid was then stained with 2% uranyl acetate. The samples were analyzed in a JEM 1011 transmission electron microscope (JEOL USA, Peabody, MA) operated at 80 kV. Digital images of 1024×1024 pixels were acquired with a CCD camera (AMT Advantage HR camera system, AMT, USA) attached to the microscope.

2.7. Oligodendrocyte culture and confocal microscopy

Spinal cord oligodendrocytes from Wistar rat 8 day old pups (Charles River Canada, St. Constant, QC) were cultured for 9 days as described previously [42]. For staining, they were fixed with 4% paraformaldehyde, permeabilized with 0.05% saponin, treated with rat anti-MBP (IgG) specific for residues Asp82-Val87 of human MBP (purchased from AbD Serotec, Raleigh, NC) and rabbit anti-α/β-tubulin (Cell Signaling Technology, Beverly, MA). After washing, donkey Cy™2-conjugated-anti-rat IgG, and donkey Cy™5-conjugated-anti-rabbit IgG (Jackson ImmunoResearch Laboratories) were added to cells. Cells were then permeabilized with 0.1% Triton X-100, treated with rhodamine-conjugated phalloidin (from Molecular Probes, Eugene, OR) and examined by confocal microscopy as described previously [42].

3. Results

3.1. Ability of modified MBP variants, bC1-P and rmC8, to cause tubulin polymerization

MBP was shown earlier by transmission electron microscopy to cause polymerization of tubulin into microtubules, and bundling of microtubules and to decrease the critical concentration to 0.69 μM [10]. Here, we show that MBP modified in vitro by phosphorylation of

bC1 at Thr94 and Thr97 (bC1-P), and pseudo-deimination to give rmC8, also caused rapid polymerization of tubulin at mole ratios of bC1 to tubulin of 1:16 to 1:4 in GPEM buffer at 37 °C, as detected by light scattering (representative experiment out of six shown for a mole ratio of 1:8 in Fig. 2A). All MBP variants polymerized tubulin equally efficiently, since the relative order of the maximum absorbance caused by the different variants, shown in the example in Fig. 2A, was not reproducible. The mean absorbance at the plateau after 30 min was 3.1 ± 0.5, 2.9 ± 0.4, and 2.5 ± 0.6 for bC1, C1-P, and rmC8, respectively ($n = 6$) and the differences were not statistically significant. The dependence on mole ratio of MBP to tubulin was also similar for the three variants (Fig. 2B). Although there could be differences in initial rate of assembly, these could not be determined with the spectrometer used. Since both Mg^{2+} and PIPES have also been reported to influence the assembly of tubulin [43,44], we also determined the effect of bC1 on tubulin light scattering in PIPES buffer lacking Mg^{2+}, and in sodium phosphate buffer with or without Mg^{2+}. A similar increase in light scattering was observed on addition of bC1 at a mole ratio to tubulin of 1:8 in these buffers as in GPEM buffer, although there was a few minutes longer lag time in sodium phosphate buffer, especially in the absence of Mg^{2+} (not shown).

3.2. Ability of bC1, bC1-P, and rmC8 to bind microtubules to LUVs

In order to determine the ability of MBP variants to bind microtubules to a negatively-charged lipid surface, paclitaxel-stabilized microtubules and MBP were added to PC/PG LUVs. The samples were centrifuged on a 40% sucrose cushion in order to separate any tubulin-MBP complex not bound to lipid from a lipid-bound MBP-tubulin complex, and from MBP-lipid or protein-free lipid vesicles. Bands and different sucrose layers were collected as shown in Fig. 1, and the amounts of lipid, tubulin, and MBP in each sample were determined. Even in the presence of a low concentration, 2 μM, of paclitaxel in the buffer, the microtubules in the absence of MBP did not completely sediment under these conditions, and were found distributed throughout the gradient. However, in the presence of MBP without LUVs (MBP to tubulin mole ratio 1:2), most of the paclitaxel-stabilized microtubules and all of the MBP sedimented as a visible pellet to the bottom of the tube for all three MBP variants, bC1, bC1-P, and rmC8, even if excess paclitaxel was not added to the buffer (Fig. 3A–C) (Table 1). Relative differences in the amount of tubulin in the pellet with the different MBP variants were not statistically significant (Table 1).

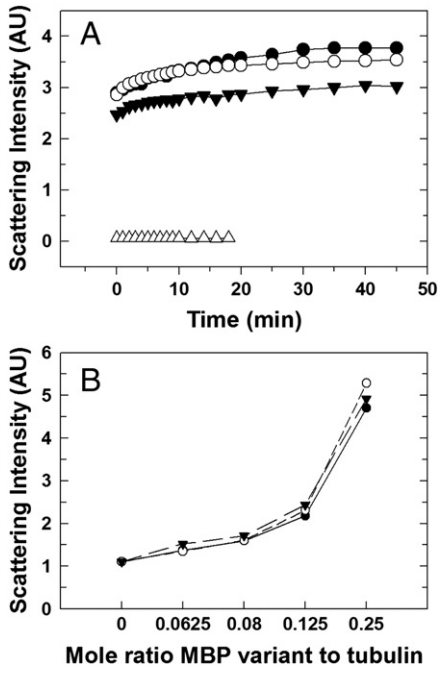

Fig. 2. (A) Increase in light scattering in arbitrary units (AU) at 340 nm with time at 37 °C due to polymerization of tubulin into microtubules, and/or bundling of microtubules, on addition of MBP variants in GPEM buffer at a 1:8 mole ratio of MBP variant to tubulin. A representative experiment from six is shown. Differences in the maximum absorbance for the three variants were not significant (see text). (B) Dependence of scattering intensity after 1 h incubation at 37 °C on mole ratio of MBP variant to tubulin. For both panels, bC1 (filled circle), bC1-P (open circle), rmC8 (closed inverted triangle), and in panel A only, GPEM buffer alone (open triangle).

The LUVs plus MBP were found as a diffuse white band in the buffer layer. Analysis of the isolated bands showed that most of the added MBP was bound to the LUVs for all three MBP variants (Fig. 3D–F), as we have reported previously [13,14]. In the presence of paclitaxel-stabilized microtubules, most of the bC1 and tubulin were found associated with some lipid in an opaque white band on top of the 40% sucrose layer (40% band), although most of the lipid was found in the buffer layer without bC1 (Fig. 3G) (Table 1). Although some tubulin is present there also, it is probably not bound to the lipid since tubulin does not bind to negatively-charged LUVs in the absence of MBP. Very little protein is found in the 40% sucrose layer below the band, or as a pellet at the bottom of the tube for LUVs with bC1 and tubulin.

The appearance of the LUVs-bC1-microtubule sample by TEM depended on how the sample was obtained and examined. If the unfractionated sample was used for TEM before centrifuging on the sucrose cushion, few free microtubules were seen, even in the presence of excess 2 μM paclitaxel (Fig. 4D; see Fig. 4A for the appearance of the microtubules used). However, the vesicles appeared very different from LUVs alone or LUVs-bC1 (see Fig. 4B for LUVs-bC1, and Fig. 4C for LUVs in the presence of only microtubules). The LUVs-bC1 are aggregated into large clumps (Fig. 4B), as expected, but still have a transparent vesicle appearance, similar to the LUVs-microtubules in the absence of bC1 (Fig. 4C). In contrast, the LUVs-bC1-microtubules look opaque and as if a polymeric intermediate of microtubules were wrapped around them (Fig. 4D,E). Binding of a protein such as MBP does not cause this appearance (Fig. 4B). This phenomenon would account for the low numbers of free microtubules in the sample of LUVs-bC1-microtubules. This suggestion is plausible, since microtubules can form a number of intermediates, such as ribbons [45], or helical filaments or linear filaments [46], which would be flexible enough to wrap around the vesicles. Previously, Seebeck et al. [47] noted that with time, the complex of a trypanosomal MAP, p60, microtubules, and liposomes also "aggregated into large impenetrable tangles".

The sample of LUVs-bC1-microtubules recovered from the band on top of the 40% sucrose cushion, however, showed some short microtubules with vesicles clearly bound to them (Fig. 4F). The larger white (unstained) vesicles in Fig. 4F may be similar to those with a wrapped appearance shown in Fig. 4D,E. A higher magnification micrograph in Fig. 4G shows some microtubules or microtubular ribbons dissociating laterally into single or double filaments, some of which appear to be wrapping around the vesicles. Some tubulin rings were also seen (not shown), indicating that the microtubules are depolymerizing to some extent under the conditions used for either centrifugation, sample collection, or TEM (although a low concentration, 2 μM, of paclitaxel was present in the buffer and sucrose used for Fig. 4D–G). Although the microtubules bound to bC1 are stable, bC1 may not be present in adequate amounts both to bind LUVS to the microtubules and to stabilize all microtubules from depolymerizing.

Because of this ambiguity, and to prevent the microtubule intermediates from wrapping around the LUVs, and enable observation of microtubules by TEM at an early stage before depolymerization occurred, a different approach was used. The bC1 was pre-incubated with paclitaxel-stabilized microtubules to allow binding, and the bC1-microtubule complex was placed directly on the grid and allowed to adsorb, as described by Moores [41]. Then LUVs were added to the

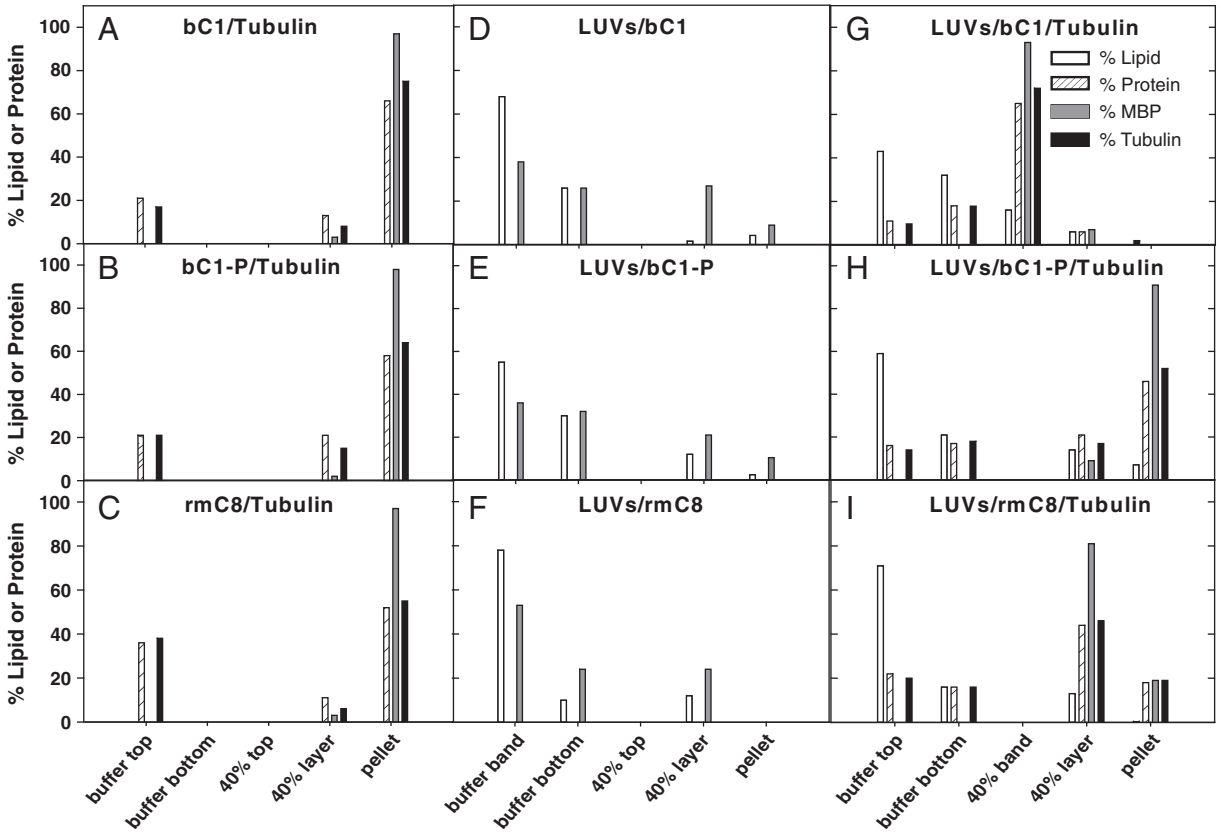

Fig. 3. Sedimentation of MBP variants with paclitaxel-stabilized microtubules alone (A–C), with LUVs alone (D–F), and with both microtubules and LUVs (G–I). The LUVs contained PC/PG 8.5/1.5 (m/m). Tubulin to MBP mole ratio was 2:1. The MBP variants were bC1 (A,D,G), bC1-P (B,E,H), rmC8 (C,F,I). Samples were centrifuged on a 40% sucrose cushion in GPEM buffer in a bench centrifuge at room temperature, and fractionated as depicted in Fig. 1. The percentage of total lipid (clear bar), protein (hatched bar), MBP variant (gray bar), and tubulin (black bar) recovered in different fractions from the tube (buffer layer, sucrose layer, pellet and any opaque bands, which were collected separately) is shown. Data in panels (A,D,G) are representative of 8 different experiments, and those in panels (B,C,E,F,H,I) are representative of 3 different experiments (see Table 1 for means and standard deviations and statistical analysis).

sample on the grid, and the grid was then stained and observed by TEM. This procedure showed LUVs clearly bound to microtubules (Fig. 5A,B, short arrows), and the LUVs had a normal appearance, as in Fig. 4B. The LUVs added to MTs on the grid without bC1 did not bind to microtubules and also looked normal (Fig. 4C). Some small ring-shaped structures were also bound to the microtubules in the presence of bC1 (long arrow in Fig. 5B). These objects are probably too small to be LUVS, and have the appearance of thick, double microtubule rings of 30–50 nm diameter, described by Devred et al. [39], and may occur as the microtubules begin to depolymerize. Thus, bC1 binds both LUVs and microtubule rings to the intact microtubules.

Neither bC1-P nor rmC8 could bind paclitaxel-stabilized microtubules to LUVs as well as bC1. Most of the bC1-P and rmC8, and over half of the tubulin, were found with only a small amount of lipid in the pellet at or near the bottom of the sucrose cushion (Fig. 3H,I) (Table 1), as in the absence of LUVs (Fig. 3B,C), and much less bC1-P,

Table 1
Distribution of lipid and protein in the 40% sucrose band and pellet.

		Percent of total lipid, MBP or tubulin					
		40% sucrose band			Pellet[a]		
Sample	n	Lipid	Tubulin	MBP[b]	Lipid	Tubulin	MBP[b]
bC1/Tubulin	8				–	80.2 ± 9.8[*]	99.6 ± 1.0[*]
bC1-P/Tubulin	3				–	74.3 ± 8.5	99.3 ± 0.9
rmC8/Tubulin	3				–	67.0 ± 11.9	97.8 ± 1.5
LUVs/bC1/Tubulin	10	31.5 ± 15.6[†]	72.5 ± 16.2[†]	87.4 ± 13.6[†]	5.6 ± 4.0	3.6 ± 8.0	5.1 ± 11.0
LUVs/bC1-P/Tubulin	3	21.7 ± 1.7	23.5 ± 13.4[††,‡]	18.8 ± 19.7[††,‡]	15.2 ± 3.8[‡]	59.2 ± 12.8[‡]	82.0 ± 25.3[‡]
LUVs/rmC8/Tubulin	3	9.5 ± 4.6[‡‡]	18.0 ± 15.6[‡]	18.7 ± 26.4[‡]	7.2 ± 4.4	59.3 ± 19.6[‡]	77.3 ± 32.0[‡]

Values represent mean ± S.D. for n different experiments. Statistical analysis was done by Student's t test.
[a] Includes material deep within the 40% layer, well below the opaque lipid–protein band that is on top of the 40% layer.
[b] MBP charge variant as indicated.
[*] $P<0.001$ for comparison of bC1/tubulin pellet with LUVs/bC1/tubulin pellet.
[†] $P<0.001$ for comparison of 40% sucrose band with pellet for LUVs/bC1/tubulin samples.
[††] $P\leq0.05$ for comparison of 40% sucrose band with pellet for LUVs/bC1-P/tubulin samples.
[‡] $P<0.001$ for comparison of 40% sucrose band of LUVs/bC1/tubulin with that for LUVs/bC1-P/tubulin or LUVs/rmC8/tubulin, or for comparison of pellet of LUVs/bC1/tubulin with that for LUVs/bC1-P/tubulin or LUVs/rmC8/tubulin.
[‡‡] $P<0.05$ for comparison of 40% sucrose band of LUVs/bC1/tubulin with that for LUVs/rmC8/tubulin.

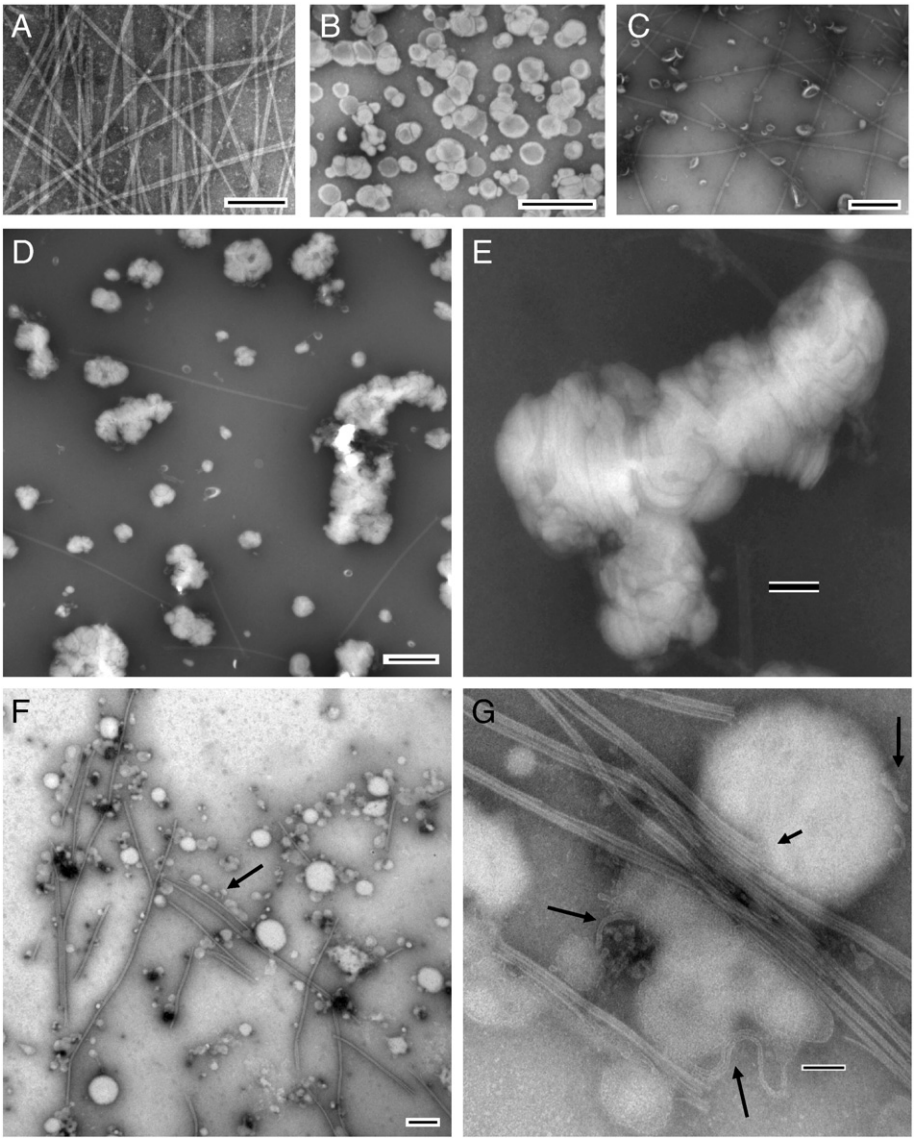

Fig. 4. Transmission electron micrographs of (A) paclitaxel-stabilized microtubules; (B) LUVs in the presence of bC1; (C) LUVs in the presence of paclitaxel-stabilized microtubules without MBP [prepared in the same way as in (Fig. 5A,B and E,F)]. Although some vesicles are next to microtubules and might be bound to them, there is much more bare surface on the microtubules than when in the presence of MBP, as in Fig. 5A,B. (D) LUVs in the presence of bC1 and microtubules before centrifugation on a 40% sucrose cushion; (E) Higher magnification of the sample used for D; (F) LUVs in the presence of bC1 and microtubules recovered in a band on top of the 40% sucrose cushion after centrifugation at room temperature. A row of LUVs bound to a short microtubule is indicated by the arrow. The larger white (unstained) vesicles may be similar to those shown in panel D; (G) Higher magnification of a large unstained vesicle from the same sample used for F. Arrows indicate some microtubule filaments which appear to be dissociating laterally from microtubules and wrapping around the vesicles. The short arrow indicates a microtubular ribbon terminating on a vesicle — the dissociated single or double filaments of the ribbon may be in contact with the vesicle and the source of some of the filaments wrapped around it. The LUVs contained PC/PG 8.5/1.5 (m/m). Samples used for panels (D–G) were prepared in the presence of excess 2 μM paclitaxel in the buffer and sucrose layer, but samples prepared in the absence of excess paclitaxel looked identical. The tubulin to bC1 mole ratio was 2:1. Bar represents 500 nm in panels (A–D,F), and 100 nm in panels (E,G).

rmC8, and tubulin were found in the lipid–protein complexes near the top of the 40% sucrose cushion, compared to bC1, for which most of the bC1 and tubulin was found in the lipid–protein band on top of the 40% sucrose, with less than 5% of these proteins in the pellet at the bottom of the tube. These differences were statistically significant ($P<0.001$) (Table 1). The TEM images of these samples, before fractionation by centrifugation on 40% sucrose, showed vesicles with the same wrapped appearance as for bC1 (Fig. 5C,D), indicating that bC1-P and rmC8 mediated binding of a microtubule intermediate to LUVs like the unmodified bC1 variant did. However, these samples also showed many unbound microtubules in contrast to samples with bC1, confirming that bC1-P and rmC8 do not bind microtubules to LUVs as well as bC1 does. The LUVs added to the complexes of bC1-P or rmC8 with paclitaxel-stabilized microtubules pre-adsorbed to a grid also were bound much less to the microtubules than observed for bC1 (Fig. 5E,F; compare to Fig. 5A,B). Many more bare microtubules can be seen in the presence of LUVs and bC1-P or rmC8 than for bC1.

3.3. Ability of bC1, bC1-P, and rmC8 to bind microtubules to actin filaments/bundles

Complexes formed by MBP variants with actin filaments (causing bundling) [13], or with microtubules, both sediment readily after low speed centrifugation, making it impossible to separate microtubules cross-linked to actin filaments/bundles via MBP from free MBP-microtubules and MBP-actin filaments/bundles. In transmission electron micrographs of negatively-stained preparations, the appearance of MBP-actin bundles is similar to that of MBP-microtubules, making it difficult to determine if MBP can cross-link actin bundles to microtubules by this technique (Fig. 6). Therefore, the ability of MBP

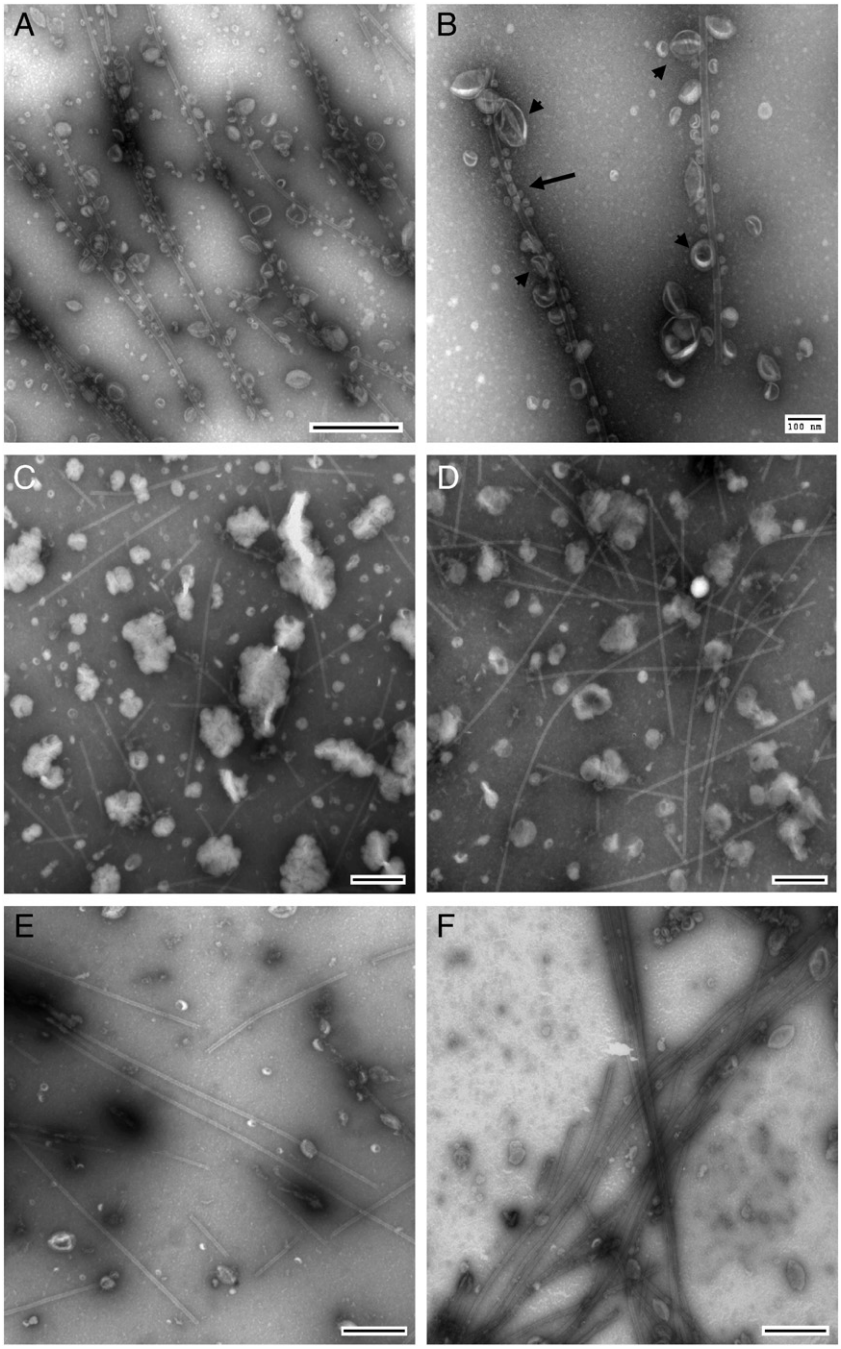

Fig. 5. Transmission electron micrographs of (A) LUVs added directly to a grid to which paclitaxel-stabilized microtubules bound to bC1 had been pre-adsorbed. The LUVs are lined up along with microtubules; (B) sample used for panel (A) at a higher magnification. Short arrows in (B) indicate LUVs bound to microtubules and long arrow indicates small structures which may be double microtubule rings bound to intact microtubules via bC1; (C) LUVs in the presence of bC1-P and paclitaxel-stabilized microtubules before centrifugation on a 40% sucrose cushion; (D) LUVs in the presence of rmC8 and paclitaxel-stabilized microtubules before centrifugation on a 40% sucrose cushion. Compare panels (C,D) here to those with bC1 prepared similarly in Fig. 4D,E; (E) LUVs added directly to a grid to which paclitaxel-stabilized microtubules bound to bC1-P had been pre-adsorbed; (F) LUVs added directly to a grid to which paclitaxel-stabilized microtubules bound to rmC8 had been pre-adsorbed. Compare E,F to those prepared similarly with bC1 in panels (A,B). Only a few bare microtubules were seen in the presence of bC1 (e.g., panels A,B), whereas many were seen in the presence of bC1-P and rmC8 (e.g., panels E,F). The LUVs contained PC/PG 8.5/1.5 (m/m). The tubulin to bC1 mole ratio was 2:1. Bar represents 500 nm in panels (A,C–F) and 100 nm in panel (B).

to cross-link actin bundles to microtubules was determined here by fluorescence microscopy using fluorescently-labeled R-actin and F-tubulin. For these experiments, a higher concentration, 20 μM, of paclitaxel was present in the GPEM buffer. This technique has been used to show that other proteins, such as doublecortin [40], the Abl-related gene tyrosine kinase [48], and the cotton kinesin GhKCH2 [49], could cross-link microtubules and actin filaments. Here, the R-actin filaments assembled in the presence of bC1 formed long fibers or compact globular appearing structures due to bundling of actin filaments by bC1 (Fig. 7A). The R-actin by itself formed filaments, which were not stained intensely but which can be seen in Fig. 7F. If the filaments aggregated into fibers or smaller globular structures, they were more intensely-stained and these structures tended to dominate the picture, as seen in Fig. 7C,D,E. Paclitaxel-stabilized F-microtubules also appeared as bundles or compact globular structures with bC1 (Fig. 7B). The F-microtubules and R-actin filaments combined without bC1 had a similar appearance as when visualized by themselves, and were not co-localized (several examples shown in

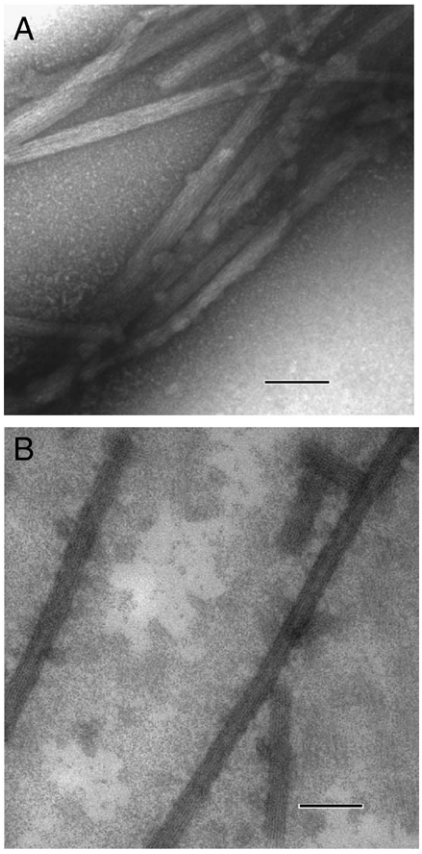

Fig. 6. Transmission electron micrographs of (A) Bundles of actin filaments in the presence of bC1 and (B) Paclitaxel-stabilized microtubules in the presence of bC1. The actin to bC1 mole ratio was 1:1 and the tubulin to bC1 ratio was 2:1. Actin bundles and microtubules bound to bC1 have similar diameter and resemble each other by TEM. Bar represents 100 nm.

Fig. 7D–F). However, in the presence of bC1, they were co-localized (Fig. 7G–L).

In the presence of bC1-P, the microtubular and actin filament structures were not as compact as in the presence of bC1 (Fig. 8A–C). Previously, bC1-P has been shown to have significantly less ability to bundle actin filaments than bC1 [12]. However, these less compact microtubule and F-actin structures were still co-localized in the presence of bC1-P. In the presence of rmC8, they were also co-localized, and appeared compact and qualitatively similar to the structures with bC1 (Fig. 8D–F). Thus, all three MBP variants were able to bind microtubules and F-actin bundles to each other.

3.4. Co-localization of MBP, actin, and tubulin in cultured oligodendrocytes (OLs)

Cultured OLs extend numerous processes which expand into large membrane sheets. Localization of MBP, actin filaments, and tubulin is shown in a partially mature OL with a mature membrane sheet on its left side and immature processes on its right side (Fig. 9). The MBP is present over the entire cell membrane (Fig. 9C). The actin cytoskeleton has been mostly lost from the mature membrane sheet, but is present in the processes along with microtubules (Fig. 9A,B,D). An example of a process in which actin filaments are located at the process tip and precede the microtubules, as seen previously for OL processes [50], is shown in Fig. 9F (arrow 1), and enlarged in Fig. 9G. In this cell process, MBP is co-localized with both actin filaments (Fig. 9E) and microtubules (Fig. 9F,G), and is co-localized with both actin and tubulin at the interface between them (Fig. 9F,G). Two processes which are expanding into a membrane leading edge (indicated by arrows 2 and 3 in Fig. 9F, and shown enlarged in Fig. 9H and I, respectively) show similar co-localization of MBP with actin filaments at the membrane edge, and with microtubules behind the actin and at the interface between them. Other examples of processes with similar colocalization of MBP with actin filaments and microtubules are shown for a less mature cell in the supplementary figure (Fig. S1).

4. Discussion

MBP was shown earlier to assemble actin and tubulin in vitro [6–10], and to bind actin filaments to a membrane surface [6,12,13]. In the present study, we show that it can also bind microtubules to a negatively-charged membrane surface, and to cross-link actin filaments to microtubules in vitro. These interactions with polyanionic proteins and surfaces are primarily electrostatic. Polylysine and polyamines can also assemble actin filaments and microtubules [51–53]. Indeed, positively-charged domains on various MAPs bind to the negatively-charged C-terminus of tubulin. This negatively-charged domain of tubulin is exposed on the surface on the outer ridges of microtubules, allowing MAPs to bind longitudinally along these outer ridges [54] and be accessible for simultaneously binding to a membrane surface or to actin filaments [55]. Actin filaments also have a high negative surface charge density due to protrusion of the negatively-charged subdomain 1 of the actin monomer along the surface of the actin filament [56]. Other MAPs, such as MAP2, can also bind to actin filaments and crosslink them to microtubules via electrostatic interactions [57]. Two trypanosomal MAPs, p60 and p15, have also been shown to bind microtubules to negatively-charged liposomes [47,58]. However, not all MAPs can behave in this way. Binding of several mammalian MAPs, MAP1B, MAP2, and tau, to microtubules is inhibited by negatively-charged liposomes because these MAPs bind preferentially to the liposomes, which displace the MAPs from the microtubules [59–61]; in some of these cases, the microtubule binding site is the same as that which binds to lipids. In the case of MBP, the basic residues are distributed throughout the entire sequence, allowing it to bind simultaneously to microtubules and LUVs or actin filaments, and cross-link these structures. Solid-state NMR spectroscopy has shown that residues throughout the entire sequence of 18.5 kDa MBP are involved in interactions with actin, although its N-terminal segment is sufficient to induce polymerization [62,63]. The polymerization and bundling of tubulin by 18.5 kDa MBP also appears to involve the entire MBP sequence [10].

Although the interaction of MBP with tubulin and actin is primarily electrostatic [10], this does not mean that it is not physiological. MBP appears to be a multifunctional protein which may serve as a scaffolding structure that tethers the cytoskeleton to the cytoplasmic surface of the plasma membrane [2,4]. Many such intrinsically disordered and multifunctional proteins are capable of association with a variety of polyanions, as reviewed in references [2,4]. MBP is such an abundant protein in OLs and myelin (10% of the total weight

Fig. 7. Confocal microscope projection images of (A) R-actin filaments (red) in the presence of bC1; (B) paclitaxel-stabilized F-microtubules (green) in the presence of bC1; (C) R-actin filaments only (long filaments are not clearly seen in this picture but can be seen in (D–F); (D–F) R-actin and F-microtubules in the absence of MBP (all merges of red and green channels); (G–L) R-actin filaments and F-microtubules in the presence of bC1; (G,J) R-actin; (H,K) F-tubulin; (I,L) merge. The actin and tubulin structures are suspended in a drop of buffer and the microscope laser beam is focused on only a thin plane (400–500 nm) in the droplet, making it difficult to detect several structures present unless they are co-localized. It is also difficult to detect the entire length of a structure unless it is within the plane examined. The GPEM buffer contained 20 μM paclitaxel. The mole ratio of actin:tubulin:bC1 was 1:4:2. Bar represents 20 μm in all panels.

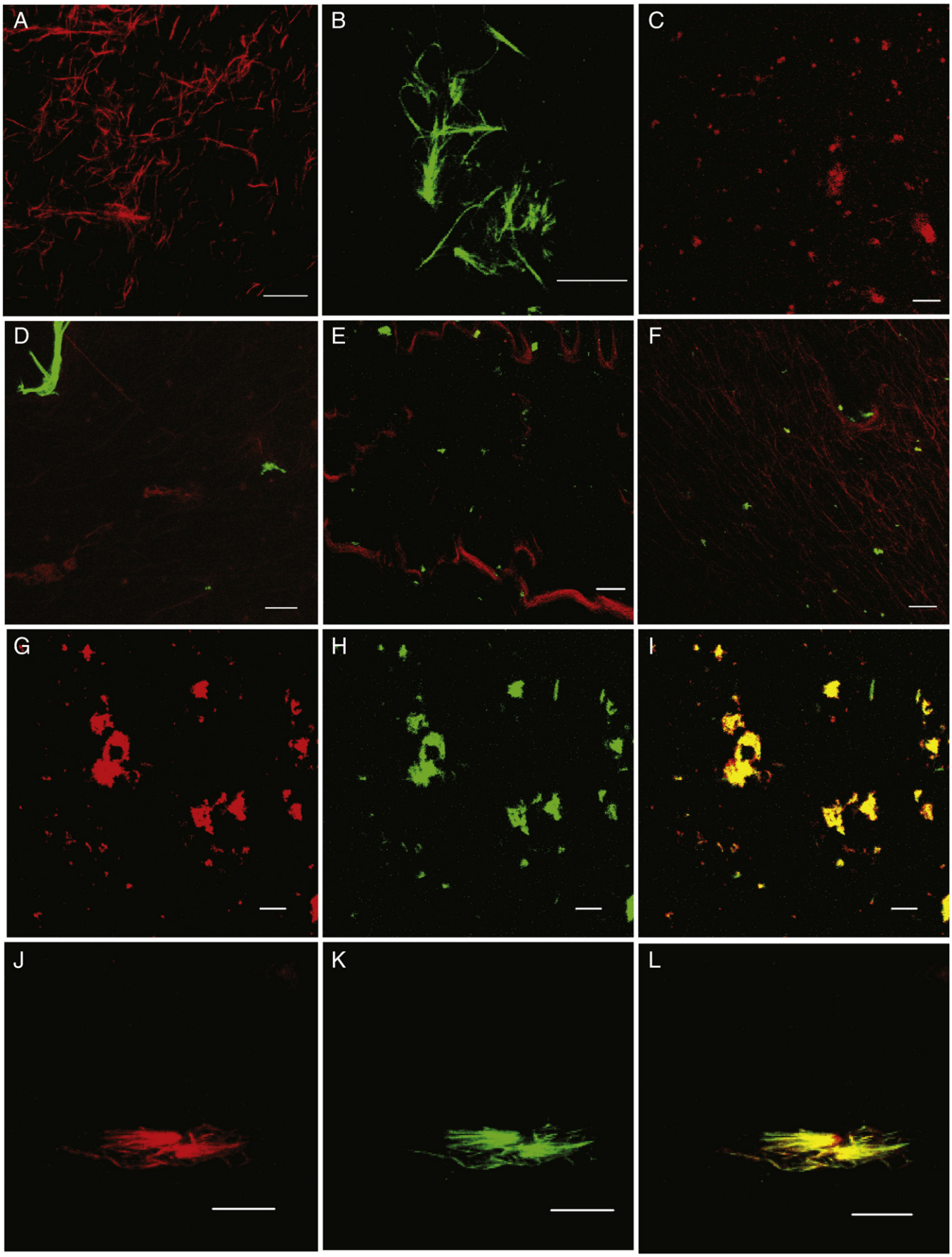
A
B
C
D
E
F
G
H
I
J
K
L

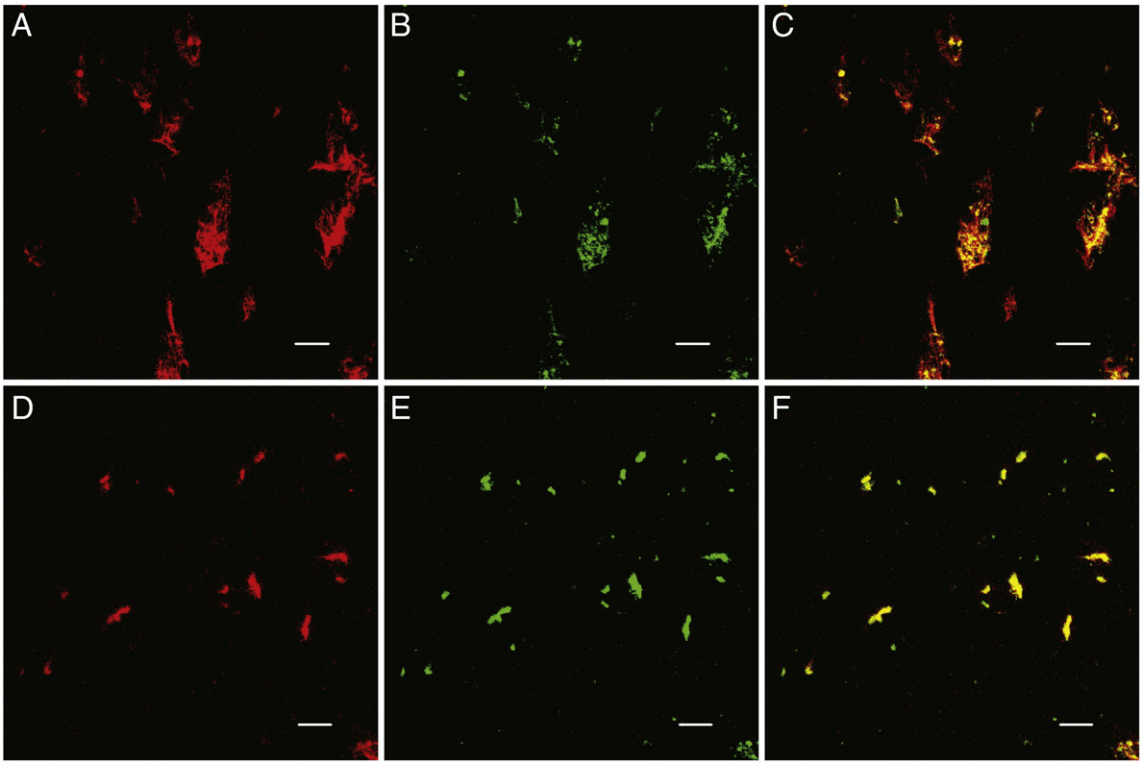

Fig. 8. Confocal microscope projection images of (A–C) R-actin filaments (red) and F-microtubules (green) in the presence of bC1-P; (D–F) R-actin filaments and F-microtubules in the presence of rmC8. (A,D) R-actin; (B,E) F-tubulin; (C,F) merge of red and green channels. The GPEM buffer contained 20 μM paclitaxel. The mole ratio of actin:tubulin:bC1-P or rmC8 was 1:4:2. Bar represents 20 μm in all panels.

of myelin), that its demonstrated ability to associate with actin and tubulin in vitro suggest that it should be able to participate in such associations in vivo also, at least at some stage of OL function. Cultured OLs produce membrane sheets containing major veins and a lacy network of cytoskeletal proteins, where actin filaments and microtubules are co-localized [64]. MBP is co-localized with these cytoskeletal veins of actin filaments and microtubules, and also with cortical actin filaments in cultured OLs. Although this does not demonstrate that they are directly associated, we have also recently shown that co-localization of over-expressed GFP-linked MBP with RFP-linked actin in immortalized N19 cells increases in ruffles and filaments induced by treatment with the phorbol ester, phorbol-12-myristate-13-acetate [65]. As in neurons, movement of the leading edge of oligodendrocyte membrane processes is driven by actin polymerization, with the microtubules located proximal to the actin network. The actin filaments precede the microtubules into the leading edge, and provide tracks for the microtubules to invade regions of new growth [50]. Associated MAPs such as tau link them [19,40]. Here, we show that MBP can also link actin filaments and microtubules in vitro, and that it appears to be co-localized in vivo in cultured oligodendrocytes with both of these networks, and at the interface between actin filaments at the leading edge and microtubules behind them. Thus, MBP may be able to link actin filaments and microtubules in these cells also, although further work is necessary to demonstrate that it binds directly to them in vivo.

Tau may participate in binding microtubules to the membrane in neuronal growth cones where very dynamic microtubules transiently extend to the tips of neurites [66]. In mature OLs, the actin filaments are lost from the periphery [17] and microtubules may reach to the tips of the processes as in neurons, where they may interact with the membrane. Tau and MBP are co-localized in the tips of OL processes [67] and both may participate in binding of microtubules to the membrane and/or to actin filaments in oligodendrocytes, as other MAPs do. In OLs from the *shiverer* mutant mouse lacking MBP, the microtubules and actin filaments were abnormal in size and distribution, and production of processes and membrane sheets was abnormal, indicating a role for MBP-cytoskeletal interactions for myelination in vivo [26]. Many myelination events, such as OL process extension, membrane sheet formation, and ensheathment of the axon depend on dynamic changes in the cytoskeleton [16,17,19,50] and MBP-cytoskeleton interactions may help regulate its dynamics. The MBP-mediated tethering of the cytoskeleton to the OL membrane may be involved in regulation of process extension and axonal ensheathment.

Post-translational modifications of MBP that reduce its net positive charge, namely phosphorylation of Thr94/Thr97 and pseudo-deimination at six sites, have been shown here to significantly decrease the ability of MBP to bind microtubules to the membrane surface, although they did not have any detectable qualitative effect on assembly of microtubules or binding of microtubules to actin filaments. These modifications were also previously shown to decrease the ability of MBP to bind actin filaments to a membrane surface, with phosphorylation having a greater effect than deimination [12,13]. The TEM showed that phosphorylation also decreased its ability to bundle actin filaments, whereas deimination had a smaller effect. These modifications had previously been shown to have only small effects on the affinity of MBP for F-actin in solution [12,13,63], but in the presence of dodecylphosphocholine micelles, pseudo-deiminated rmC8 had less affinity for F-actin than rmC1, and a decreased ability to polymerize and bundle actin filaments [63]. Possibly phosphorylation of MBP at other sites [2,33] affects its ability to assemble and bind to microtubules, since naturally occurring charge components of MBP, which are partially phosphorylated at a number of Ser/Thr residues, were more effective at assembling microtubules than the unmodified form bC1 [10].

Phosphorylation and deimination of MBP did not significantly affect its binding to lipid vesicles under the conditions used, although these modifications may decrease the affinity of MBP for a lipid

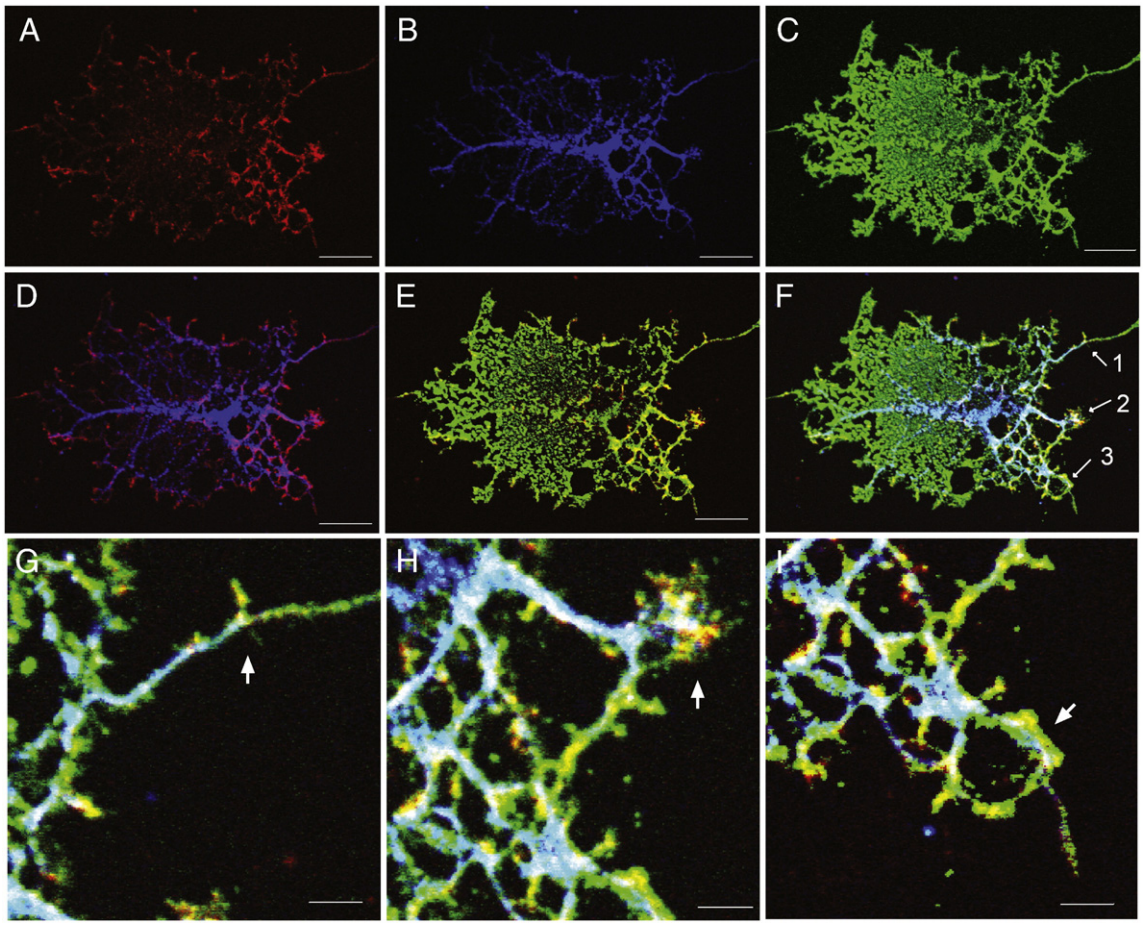

Fig. 9. Confocal microscope projection images of a partially mature OL with a membrane sheet on the left side and membrane processes on the right side, stained with (A) phalloidin to stain actin filaments, red; (B) anti-α/βtubulin, blue; (C) anti-MBP, green; (D) merge of panels (A and B) showing co-localization (purple) of tubulin (blue) and actin (red); (E) merge of panels (A and C) showing co-localization (yellow) of actin (red) and MBP (green); (F) merge of panels (A,B,C) showing co-localization of actin, tubulin, and MBP (white), tubulin and MBP (aqua), MBP and actin (yellow), and actin and tubulin (purple); (G–I) enlargements of areas in panel (F) marked by white arrows (1,2,3), respectively, showing processes (white arrows) where actin and MBP are co-localized at the tip (yellow), with tubulin and MBP co-localized behind (aqua), and actin, MBP, and tubulin co-localized (white areas) at the interface of the actin microfilaments and the microtubules. In this cell, most of the cytoskeleton has been lost in the mature membrane sheet, whereas the narrow processes, with areas where membrane sheet formation is beginning, contain actin filaments and microtubules. Bar represents 20 μm in panels (A–F), and 5 μm in panels (G–I).

surface. However, the complexes of bC1-P and rmC8 with microtubules were significantly less bound to lipid vesicles than that of bC1 with microtubules, suggesting that these modified forms bound preferentially to microtubules over the lipid vesicles. Negatively-charged actin filaments were shown to bind less to lipid vesicles as the negative surface charge of the lipid vesicles increased due to either an increase in the ratio of negatively-charged lipid to neutral PC or to phosphorylation or deimination of MBP [6,12,13], suggesting that they are repelled from the negatively-charged lipid surface. The less positively-charged bC1-P and rmC8 would also be less effective at neutralizing the charge on the microtubules than bC1, so that the negatively-charged complex with microtubules would be repelled from the surface of the negatively-charged lipid vesicles. Although the ratios of bC1-P and rmC8 to tubulin are higher in the dissociated complex found in the pellet than in the lipid-protein band (Table 1), it is not known how much MBP is on the surface of microtubular bundles, and how much is within the bundles involved in crosslinking the microtubules. The latter interaction would not contribute much to reduction of the surface charge of the bundles.

These associations of MBP with the cytoskeleton may allow it to play roles in signaling in OLs and in compact myelin, which also contains actin and tubulin [4,68]. These proteins may be associated in myelin with a series of tight junctions, called radial component, passing through many layers of the myelin sheath [23]. They may facilitate inter-myelin-axonal communication and MBP may participate in this through its interactions with actin and tubulin, in addition to proteins with SH3 domains.

Supplementary data to this article can be found online at doi:10.1016/j.bbamem.2010.12.016.

Acknowledgement

This work was supported by an operating grant to JMB and GH from the Canadian Institutes of Health Research, MOP 86483.

References

[1] G. Harauz, N. Ishiyama, C.M.D. Hill, I.R. Bates, D.S. Libich, C. Farès, Myelin basic protein — diverse conformational states of an intrinsically unstructured protein and its roles in myelin assembly and multiple sclerosis, Micron 35 (2004) 503–542.
[2] G. Harauz, V. Ladizhansky, J.M. Boggs, Structural polymorphism and multifunctionality of myelin basic protein, Biochemistry 48 (2009) 8094–8104.
[3] V.N. Uversky, A.K. Dunker, Understanding protein non-folding, Biochim. Biophys. Acta 1804 (2010) 1231–1264.
[4] J.M. Boggs, Myelin basic protein: a multifunctional protein, Cell. Mol. Life Sci. 63 (2006) 1945–1961.
[5] D.S. Libich, C.M.D. Hill, I.R. Bates, F.R. Hallett, S. Armstrong, A. Siemiarczuk, G. Harauz, Interaction of the 18.5-kD isoform of myelin basic protein with Ca2+-calmodulin: effects of deimination assessed by intrinsic Trp fluorescence spectroscopy, dynamic light scattering, and circular dichroism, Protein Sci. 12 (2003) 1507–1521.
[6] J.M. Boggs, G. Rangaraj, Interaction of lipid-bound myelin basic protein with actin filaments and calmodulin, Biochemistry 39 (2000) 7799–7806.

[7] Z. Dobrowolski, H. Osinska, M. Mossakowska, B. Barylko, Ca^{2+}-calmodulin-dependent polymerization of actin by myelin basic protein, Eur. J. Cell Biol. 42 (1986) 17–26.
[8] C.M.D. Hill, G. Harauz, Charge effects modulate actin assembly by classic myelin basic protein isoforms, Biochem. Biophys. Res. Commun. 329 (2005) 362–369.
[9] N.M. Modesti, H.S. Barra, The interaction of myelin basic protein with tubulin and the inhibition of tubulin carboxypeptidase activity, Biochem. Biophys. Res. Commun. 136 (1986) 482–489.
[10] C.M.D. Hill, D.S. Libich, G. Harauz, Assembly of tubulin by classic myelin basic protein isoforms and regulation by post-translational modification, Biochemistry 44 (2005) 16672–16683.
[11] E. Polverini, G. Rangaraj, D.S. Libich, J.M. Boggs, G. Harauz, Binding of the proline-rich segment of myelin basic protein to SH3-domains — spectroscopic, microarray, and modelling studies of ligand conformation and effects of post-translational modifications, Biochemistry 47 (2008) 267–282.
[12] J.M. Boggs, G. Rangaraj, W. Gao, Y.M. Heng, Effect of phosphorylation of myelin basic protein by MAPK on its interactions with actin and actin binding to a lipid membrane *in vitro*, Biochemistry 45 (2006) 391–401.
[13] J.M. Boggs, G. Rangaraj, C.M.D. Hill, I.R. Bates, Y.M. Heng, G. Harauz, Effect of arginine loss in myelin basic protein, as occurs in its deiminated charge isoform, on mediation of actin polymerization and actin binding to a lipid membrane *in vitro*, Biochemistry 44 (2005) 3524–3534.
[14] L. Homchaudhuri, E. Polverini, W. Gao, G. Harauz, J.M. Boggs, Influence of membrane surface charge and post-translational modifications to myelin basic protein on its ability to tether the Fyn-SH3 domain to a membrane *in vitro*, Biochemistry 48 (2009) 2385–2393.
[15] F. Pirollet, J. Derancourt, J. Haiech, D. Job, R.L. Margolis, Ca(2+)-calmodulin regulated effectors of microtubule stability in bovine brain, Biochemistry 31 (1992) 8849–8855.
[16] M.R. Galiano, A. Andrieux, J.C. Deloulme, C. Bosc, A. Schweitzer, D. Job, M.E. Hallak, Myelin basic protein functions as a microtubule stabilizing protein in differentiated oligodendrocytes, J. Neurosci. Res. 84 (2006) 534–541.
[17] R. Wilson, P.J. Brophy, Role for the oligodendrocyte cytoskeleton in myelination, J. Neurosci. Res. 22 (1989) 439–448.
[18] M.R. Galiano, C. Lopez Sambrooks, M.E. Hallak, Insights into the interaction of myelin basic protein with microtubules, in: J.M. Boggs (Ed.), Myelin Basic Protein, Intrinsically Disordered Proteins, Nova Science Publishers, New York, 2008, pp. 129–147.
[19] C. Richter-Landsberg, Organization and functional roles of the cytoskeleton in oligodendrocytes, Microsc. Res. Tech. 52 (2001) 628–636.
[20] M. Taketomi, N. Kinoshita, K. Kimura, M. Kitada, T. Noda, H. Asou, T. Nakamura, C. Ide, Nogo-A expression in mature oligodendrocytes of rat spinal cord in association with specific molecules, Neurosci. Lett. 332 (2002) 37–40.
[21] F. Kozielski, T. Riaz, S. Debonis, C.J. Koehler, M. Kroening, I. Panse, M. Strozynski, I. M. Donaldson, B. Thiede, Proteome analysis of microtubule-associated proteins and their interacting partners from mammalian brain, Amino Acids (in press) online 2 June (doi:10.1007/s00726-010-0649-5).
[22] D.N. Arvanitis, W. Min, Y. Gong, Y.M. Heng, J.M. Boggs, Two types of detergent-insoluble, glycosphingolipid/cholesterol-rich membrane domains from isolated myelin, J. Neurochem. 94 (2005) 1696–1710.
[23] J. Karthigasan, B. Kosaras, J. Nguyen, D.A. Kirschner, Protein and lipid composition of radial component-enriched CNS myelin, J. Neurochem. 62 (1994) 1203–1213.
[24] C.S. Gillespie, R. Wilson, A. Davidson, P.J. Brophy, Characterization of a cytoskeletal matrix associated with myelin from rat brain, Biochem. J. 260 (1989) 689–696.
[25] P.M. Pereyra, E. Horvath, P.E. Braun, Triton X-100 extractions of central nervous system myelin indicate a possible role for the minor myelin proteins in the stability in lamellae, Neurochem. Res. 13 (1988) 583–595.
[26] C.A. Dyer, T.M. Philibotte, S. Billings-Gagliardi, M.K. Wolf, Cytoskeleton in myelin-basic-protein-deficient shiverer oligodendrocytes, Dev. Neurosci. 17 (1995) 53–62.
[27] N. Murray, A.J. Steck, Impulse conduction regulates myelin basic protein phosphorylation in rat optic nerve, J. Neurochem. 43 (1984) 243–248.
[28] C.M. Atkins, M. Yon, N.P. Groome, J.D. Sweatt, Regulation of myelin basic protein phosphorylation by mitogen-activated protein kinase during increased action potential firing in the hippocampus, J. Neurochem. 73 (1999) 1090–1097.
[29] C.A. Dyer, T.M. Philibotte, M.K. Wolf, S. Billings-Gagliardi, Myelin basic protein mediates extracellular signals that regulate microtubule stability in oligodendrocyte membrane sheets, J. Neurosci. Res. 39 (1994) 97–107.
[30] T. Vartanian, S. Szuchet, G. Dawson, A.T. Campagnoni, Oligodendrocyte adhesion activates protein kinase C-mediated phosphorylation of myelin basic protein, Science 234 (1986) 1395–1398.
[31] B. Soliven, M. Takeda, S. Szuchet, Depolarizing agents and tumor necrosis factor-alpha modulate protein phosphorylation in oligodendrocytes, J. Neurosci. Res. 38 (1994) 91–100.
[32] D.D. Wood, M.A. Moscarello, The isolation, characterization, and lipid-aggregating properties of a citrulline containing myelin basic protein, J. Biol. Chem. 264 (1989) 5121–5127.
[33] J.K. Kim, F.G. Mastronardi, D.D. Wood, D.M. Lubman, R. Zand, M.A. Moscarello, Multiple sclerosis: an important role for post-translational modifications of myelin basic protein in pathogenesis, Mol. Cell. Proteomics 2 (2003) 453–462.
[34] M.A. Moscarello, D.D. Wood, C. Ackerley, C. Boulias, Myelin in multiple sclerosis is developmentally immature, J. Clin. Invest. 94 (1994) 146–154.
[35] S. Cheifetz, M.A. Moscarello, C.M. Deber, NMR investigation of the charge isomers of bovine myelin basic protein, Arch. Biochem. Biophys. 233 (1984) 151–160.
[36] I.R. Bates, D.S. Libich, D.D. Wood, M.A. Moscarello, G. Harauz, An Arg/Lys−>Gln mutant of recombinant murine myelin basic protein as a mimic of the deiminated form implicated in multiple sclerosis, Protein Expr. Purif. 25 (2002) 330–341.
[37] I.R. Bates, P. Matharu, N. Ishiyama, D. Rochon, D.D. Wood, E. Polverini, M.A. Moscarello, N.J. Viner, G. Harauz, Characterization of a recombinant murine 18.5-kDa myelin basic protein, Protein Expr. Purif. 20 (2000) 285–299.
[38] J.M. Boggs, N. Samji, M.A. Moscarello, G.A. Hashim, E.D. Day, Immune lysis of reconstituted myelin basic protein–lipid vesicles and myelin vesicles, J. Immunol. 130 (1983) 1687–1694.
[39] F. Devred, P. Barbier, S. Douillard, O. Monasterio, J.M. Andreu, V. Peyrot, Tau induces ring and microtubule formation from αβ-tubulin dimers under nonassembly conditions, Biochemistry 43 (2004) 10520–10531.
[40] M. Tsukada, A. Prokscha, E. Ungewickell, G. Eichele, Doublecortin association with actin filaments is regulated by neurabin II, J. Biol. Chem. 280 (2005) 11361–11368.
[41] C. Moores, Studying microtubules by electron microscopy, Meth. Cell Biol. 88 (2008) 299–317.
[42] J.M. Boggs, H. Wang, Co-clustering of galactosylceramide and membrane proteins in oligodendrocyte membranes on interaction with polyvalent carbohydrate and prevention by an intact cytoskeleton, J. Neurosci. Res. 76 (2004) 342–355.
[43] S. Roychowdhury, F. Gaskin, Magnesium requirements for guanosine 5′-O-(3-thiotriphosphate) induced assembly of microtubule protein and tubulin, Biochemistry 25 (1986) 7847–7853.
[44] P.G. Waxman, A.A. del Campo, M.C. Lowe, E. Hamel, Induction of polymerization of purified tubulin by sulfonate buffers. Marked differences between 4-morpholineethanesulfonate (Mes) and 1, 4-piperazineethanesulfonate (Pipes), Eur. J. Biochem. 120 (1981) 129–136.
[45] I.V. Sandoval, K. Weber, Different tubulin polymers are produced by microtubule-associated proteins MAP2 and tau in the presence of guanosine 5′-(alpha, beta-methylene)triphosphate, J. Biol. Chem. 255 (1980) 8952–8954.
[46] E.A. Weinhofer, J.L. Travis, Evidence for a direct conversion between two tubulin polymers, microtubules and helical filaments, in the foraminiferan, Allogromia laticollaris, Cell Motil. Cytoskeleton 41 (1998) 107–116.
[47] T. Seebeck, V. Kung, T. Wyler, M. Muller, A 60-kDa cytoskeletal protein from *Trypanosoma brucei brucei* can interact with membranes and with microtubules, Proc. Natl. Acad. Sci. U. S. A 85 (1988) 1101–1104.
[48] A.L. Miller, Y. Wang, M.S. Mooseker, A.J. Koleske, The Abl-related gene (Arg) requires its F-actin-microtubule cross-linking activity to regulate lamellipodial dynamics during fibroblast adhesion, J. Cell Biol. 165 (2004) 407–419.
[49] T. Xu, Z. Qu, X. Yang, X. Qin, J. Xiong, Y. Wang, D. Ren, G. Liu, A cotton kinesin GhKCH2 interacts with both microtubules and microfilaments, Biochem. J. 421 (2009) 171–180.
[50] J. Song, B.D. Goetz, P.W. Baas, I.D. Duncan, Cytoskeletal reorganization during the formation of oligodendrocyte processes and branches, Mol. Cell. Neurosci. 17 (2001) 624–636.
[51] M.R. Mejillano, R.H. Himes, Assembly properties of tubulin after carboxyl group modification, J. Biol. Chem. 266 (1991) 657–664.
[52] J.X. Tang, P.A. Janmey, The polyelectrolyte nature of F-actin and the mechanism of actin bundle formation, J. Biol. Chem. 271 (1996) 8556–8563.
[53] P. Savarin, A. Barbet, S. Delga, V. Joshi, L. Hamon, J. Lefevre, S. Nakib, J.P. De Bandt, C. Moinard, P.A. Curmi, D. Pastre, A central role for polyamines in microtubule assembly in cells, Biochem. J. 430 (2010) 151–159.
[54] J. Al-Bassam, R.S. Ozer, D. Safer, S. Halpain, R.A. Milligan, MAP2 and tau bind longitudinally along the outer ridges of microtubule protofilaments, J. Cell Biol. 157 (2002) 1187–1196.
[55] J. Wolff, Plasma membrane tubulin, Biochim. Biophys. Acta 1788 (2009) 1415–1433.
[56] T.E. Angelini, R. Golestanian, R.H. Coridan, J.C. Butler, A. Beraud, M. Krisch, H. Sinn, K.S. Schweizer, G.C. Wong, Counterions between charged polymers exhibit liquid-like organization and dynamics, Proc. Natl Acad. Sci. USA 103 (2006) 7962–7967.
[57] B. Pedrotti, R. Colombo, K. Islam, Interactions of microtubule-associated protein MAP2 with unpolymerized and polymerized tubulin and actin using a 96-well microtiter plate solid-phase immunoassay, Biochemistry 33 (1994) 8798–8806.
[58] R. Rasooly, N. Balaban, Structure of p15 trypanosome microtubule associated protein, Parasitol. Res. 88 (2002) 1034–1039.
[59] E. Yamauchi, K. Titani, H. Taniguchi, Specific binding of acidic phospholipids to microtubule-associated protein MAP1B regulates its interaction with tubulin, J. Biol. Chem. 272 (1997) 22948–22953.
[60] C.D. Surridge, R.G. Burns, Phosphatidylinositol inhibits microtubule assembly by binding to microtubule-associated protein 2 at a single, specific, high-affinity site, Biochemistry 31 (1992) 6140–6144.
[61] T.B. Shea, Phospholipids alter tau conformation, phosphorylation, proteolysis, and association with microtubules: implication for tau function under normal and degenerative conditions, J. Neurosci. Res. 50 (1997) 114–122.
[62] M.A.M. Ahmed, V.V. Bamm, L. Shi, M. Steiner-Mosonyi, J.F. Dawson, L. Brown, G. Harauz, V. Ladizhansky, Induced secondary structure and polymorphism in an intrinsically disordered structural linker of the CNS: solid-state NMR and FTIR spectroscopy of myelin basic protein bound to actin, Biophys. J. 96 (2009) 180–191.
[63] V.V. Bamm, M.A. Ahmed, G. Harauz, Interaction of myelin basic protein with actin in the presence of dodecylphosphocholine micelles, Biochemistry 49 (2010) 6903–6915.
[64] C.A. Dyer, J.A. Benjamins, Organization of oligodendroglial membrane sheets. I: Association of myelin basic protein and 2′, 3′-cyclic nucleotide 3′-phosphohydrolase with cytoskeleton, J. Neurosci. Res. 24 (1989) 201–211.
[65] G.S.T. Smith, L.M. Petley-Ragan, W. Gao, J.M. Boggs, G. Harauz, Classic isoforms of myelin basic protein associate with the cytoskeleton in oligodendroglial cells

during ruffling, Transactions of the American Society for Neurochemistry 41st Annual Meeting, 2010,, OP05-01.
[66] R. Brandt, J. Leger, G. Lee, Interaction of tau with the neural plasma membrane mediated by tau's amino-terminal projection domain, J. Cell Biol. 131 (1995) 1327–1340.
[67] P. LoPresti, S. Szuchet, S.C. Papasozomenos, R.P. Zinkowski, L.I. Binder, Functional implications for the microtubule-associated protein tau: localization in oligodendrocytes, Proc. Natl Acad. Sci. USA 92 (1995) 10369–10373.
[68] J.M. Boggs, Myelin Basic Protein, Nova Science Publishers, Hauppauge, NY, 2008.